JOURNAL OF MODERN OPTICS, 2003, 1–8, preview article

Combined amplitude and phase filters for increased tolerance to spherical aberration

SAMIR MEZOUARI and ANDREW R. HARVEY

Electronic, Electrical and Computer Engineering, School of Engineering and Physical Sciences, Heriot-Watt University, Riccarton, EH14 4AS, Edinburgh, UK

(*Received 30 September 2002; revision received 28 January 2003*)

Abstract. Analysis of the expression for Strehl ratio for a circularly symmetric pupil allows one to design complex filters that offer reduced sensitivity to spherical aberration. It is shown that filters that combine hyper-Gaussian amplitude transmittance with hyper-Gaussian phase modulation provide five-fold reduction in sensitivity to spherical aberration. Furthermore, this is achieved without the introduction of zeros into the modulation transfer function and deconvolution can restore the transfer function to that of a diffraction-limited imager. The performance of the derived combined amplitude and phase filter is illustrated through the variation of its axial intensity versus spherical aberration. This technique is applicable to imaging in the presence of significant amounts of spherical aberration as is encountered in, for example, microscopy.

1. Introduction

Optical aberrations denote the departure of imaging systems from the idealized conditions of Gaussian optics. An extensive literature is devoted to the alleviation of defocus and the reduction of the effects of residual aberrations. In this paper, we restrict investigation to spherical aberration (SA) only. The effects of SA are well known. For instance, in confocal microscopy, the SA introduced by weakly aberrating media can considerably degrade imaging performance [1], and recently [2] it has been shown that for small Fresnel number focusing systems, SA can increase the maximum intensity at the focal point. Alleviation of aberrations has previously been described using amplitude-only filters or phase-only filters placed in front of the aberrated imaging system to produce a specific axial response that reduces sensitivity to optical aberrations [3–12]. Ojeda-Castaneda *et al*. [7–11] demonstrated the performance achieved by various amplitude filters to extend the depth of focus or to reduce the effect of SA, but to the detriment of light gathering power. For applications where efficient light throughput is essential, the use of phase-only filters has been reported [13–15]. We report here derivation of a new filter that employs amplitude and phase modulation to reduce sensitivity to SA.

Principle contact Dr Andy Harvey: E-mail: a.r.harvey@hw.ac.uk, Tel.: +44(0) 131 451 3356, Fax: +44 (0)131 451 3327

Journal of Modern Optics ISSN 0950–0340 print/ISSN 1362–3044 online © 2003 Taylor & Francis Ltd
http://www.tandf.co.uk/journals
DOI: 10.1080/0950034031000099205

In the Debye approximation, the intensity of a circularly-symmetric system that suffers from defocus, W_{20}, and SA, W_{40}, measured in units of wavelength, is given by [8]:

$$I(W_{20},\ W_{40}) = 4\pi^2 \left| \int_0^{\infty} \tilde{p}(\rho) \exp\left[\mathrm{i}2\pi\left\{W_{20}(\rho/\rho_0)^2 + W_{40}\,(\rho/\rho_0)^4\right\}\right] \rho\,\mathrm{d}p \right|^2, \qquad (1)$$

where ρ is the radial spatial frequency whose maximum value is the cutoff frequency, ρ_0. The axially symmetric generalized pupil function, $\tilde{p}(\rho)$, is complex within $0 \leqslant \rho \leqslant \rho_0$, and zero elsewhere. When the optical system is well focused, $W_{20} \approx 0$, and the on-axis intensity in equation (1) can be rewritten, with a convenient change of variables, as a Fourier-transform operation:

$$I\,(W_{20} = 0,\ W_{40}) = I(W_{40}) = \pi^2 \frac{\rho_0^4}{4} \left| \int_{-\infty}^{\infty} Q(\xi) \exp\left[\mathrm{i}2\pi W_{40}\xi\right] \mathrm{d}\xi \right|^2, \qquad (2)$$

where

$$\xi = (\rho/\rho_0)^4 - 1/2; \qquad \tilde{p}(\rho) = (\rho/\rho_0)^2 Q(\xi). \qquad (3)$$

The complex function, $Q(\xi)$, is null when ξ is outside the interval $-1/2 \leqslant \xi \leqslant 1/2$. The expression for the intensity at the focal point is thus reduced to a simple Fourier transform of the function Q. To derive the pupil function that reduces the variation of the intensity at the focal point, $I(W_{40})$, with respect to SA, W_{40}, we use the stationary phase approximation to evaluate equation (2). Therefore, the intensity can be rewritten as

$$I(W_{40}) = \pi^2 \frac{\rho_0^4}{4} \frac{(A(\xi_s))^2}{|\theta''(\xi_s)|}, \qquad (4)$$

where

$$Q(\xi) = A(\xi) \exp\left[\mathrm{i}2\pi\theta(\xi)\right]. \qquad (5)$$

The modulus of the complex function $Q(\xi)$ is given by $A(\xi)$, the function $\theta(\xi)$ represents the phase delay introduced by the optical element, and ξ_s is the stationary point. To ensure invariance to SA, the intensity $I(W_{40})$ must satisfy the following relation:

$$\frac{\partial I(W_{40})}{\partial W_{40}} = 0. \qquad (6)$$

Let us consider first the simple case where $A(\xi) = 1$. Replacing equation (4) in equation (6), and by integrating the resulting differential equation, we obtain the expression for the phase delay:

$$\theta(\xi) = \alpha\xi^2, \qquad (7)$$

where $\alpha \neq 0$ is a real.

By substituting equation (7) into equation (5), the pupil function in equation (3) is, therefore, given by

$$\tilde{p}(\rho) = (\rho/\rho_0)^2 \exp\left[\mathrm{i}2\pi\alpha((\rho/\rho_0)^4 - 1/2)^2\right]. \qquad (8)$$

The quadratic term in the amplitude of the pupil function represents attenuation of light at the centre of the aperture producing a graduated annular aperture, while the phase function includes an eighth-order term. The performance of the complex filter in equation (8) is shown in figure 1 where the variation of the intensity near the focal point with W_{40} is compared with that of an ideal lens. In this and subsequent graphs of focal-point intensity distributions, intensity is normalized with respect to the peak of the diffraction-limited point-spread function and the indicated scaling factor is therefore equivalent to the Strehl ratio. According to Rayleigh's criterion, the normalized intensity of 0.8 represents the lower limit to low aberration imaging. The derived filter displays a high tolerance to SA and the limits for low aberration imaging are extended from $W_{40} = \pm 0.25$ for an ideal lens up to ± 1.4 when $\alpha = 0.75\,\pi$. Although the complex filter in equation (8) achieves an improvement in tolerance to SA, the light transmitted is considerably reduced because of the low transmittance of the filter. The quadratic variation in amplitude

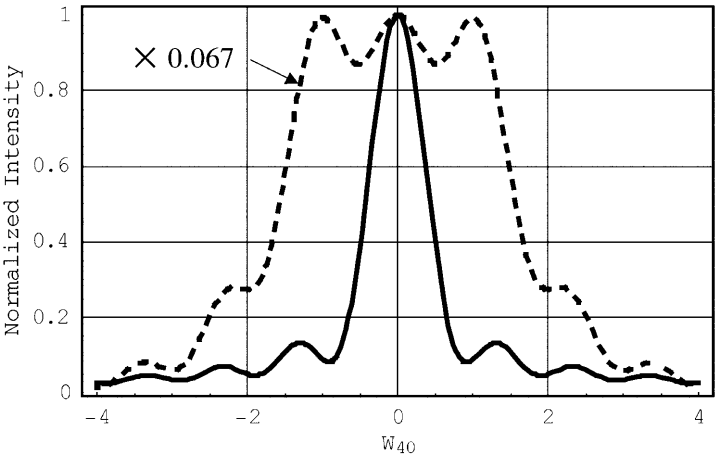

Figure 1. Intensity normalized with respect to a diffraction-limited peak intensity at the focal point versus spherical aberration W_{40} for a simple lens (——) and the complex filter (- - - -). The relative intensity scaling for the complex filter is indicated.

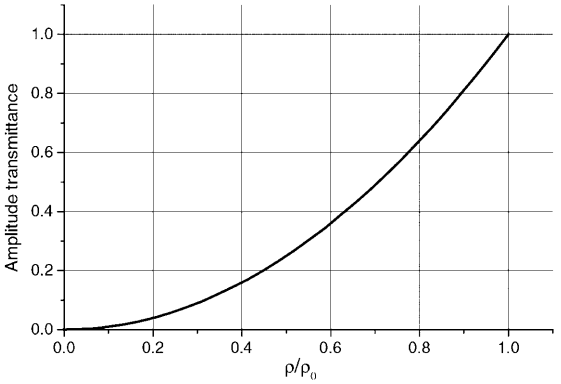

Figure 2. Amplitude transmittance of the complex filter, equation (8), as a function of the normalized radial coordinate.

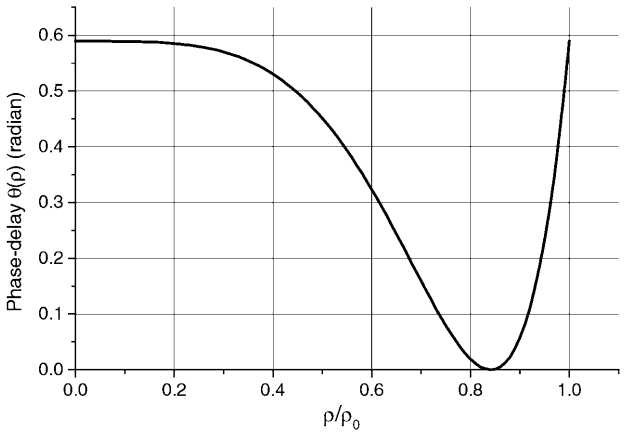

Figure 3. The variation of the phase-delay function, $\theta(\rho)$, as a function of the normalized radial coordinate.

transmittance is shown in figure 2 and the phase–delay function $\theta(\xi)$ is displayed in figure 3.

The reduction of light throughput is an important issue when such combined amplitude and phase filters are employed. The expression of light throughput normalized to the full aperture is given by[10]

$$T = 2\pi \int_0^{\rho_0} |\tilde{p}(\rho)|^2 \rho \, \mathrm{d}\rho / \pi \rho_0^2. \tag{9}$$

Thus, by substituting equation (8) in equation (9), we deduce that the light throughput is reduced by a factor of 1/3 relative to the full aperture. The dominant contribution to the effects of SA arises from contributions from the central part of the pupil, therefore it is reasonable to expect that only modest degradation in SA sensitivity will arise from the heuristic approach of increasing the transmittance of the pupil close to its periphery to unity. We therefore define a new pupil function

$$\tilde{p}(\rho) = \begin{cases} a(\rho/\rho_0)^2 \exp[\mathrm{i}2\pi\alpha((\rho/\rho_0)^4 - 1/2)^2] & \text{if } a(\rho/\rho_0)^2 \leqslant 1, \\ \exp[\mathrm{i}2\pi\alpha((\rho/\rho_0)^4 - 1/2)^2] & \text{if } a(\rho/\rho_0)^2 > 1, \end{cases} \tag{10}$$

where $a \geqslant 1$ is a real. This is depicted in figure 4. When $a = 1$, the relation (10) is identical to equation (8).

The variation of light throughput, as shown in figure 5, can be increased by a factor of up to 2 when the parameter $a = 3$. However, the performance achieved by the filter, as given by the variation of axial intensity with W_{40} is diminished as shown in figure 6. For instance, when $a = 1.5$ the complex filter alleviates only the positive SA, while for $a = 3$ the range of W_{40} over which the normalized axial intensity remains above 0.8 is only about twice (2.1) that of an ideal lens. An alternative heuristic approach is the use of a hyper-Gaussian transmittance in which the pupil function is given by

$$\tilde{p}(\rho) = c(\rho/\rho_0)^2 \exp[-\beta((\rho/\rho_0)^4 - 1/2)^2] \exp[\mathrm{i}2\pi\alpha((\rho/\rho_0)^4 - 1/2)^2], \tag{11}$$

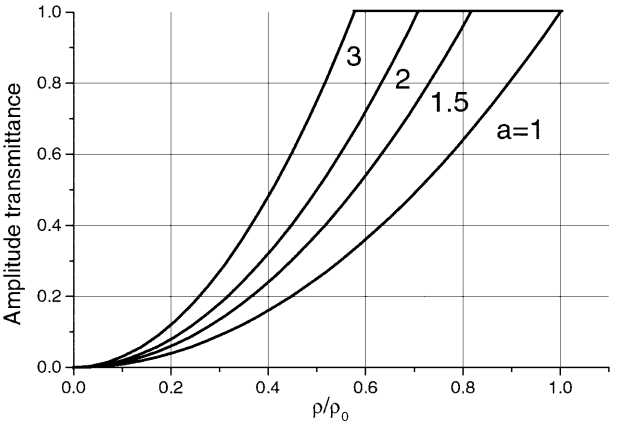

Figure 4. Transmittance of semi-shaded complex filters, relation (10), as a function of the normalized radial coordinate for different values of the parameter $a = 1$, 1.5, 2, and 3.

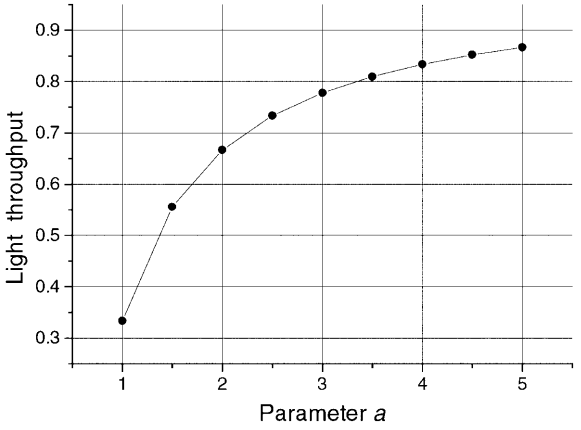

Figure 5. The light throughput (normalized to full-aperture) of semi-shaded complex filters as function of the obscuration parameter a.

where β is a positive real and c is a constant of normalization. Numerical computation (by replacing equation (11) in equation (9)) demonstrates that a maximum light throughput of about 0.432 is attained when $\beta = 1.3$. This filter exhibits an improvement of 30% in light throughput in comparison with equation (8). The transmittance of the hyper-Gaussian complex filter (11) is shown in figure 7 while its performance is slightly enhanced as displayed in figure 8.

To complete this study and in order to appreciate the performance achieved by the hyper-Gaussian filters, we display in figure 9 and figure 10 a comparison between the computed modulation transfer function (MTF) for different values of SA. The MTF of a perfect lens is sensitive to the variation of the amount of additional SA as shown in figure 9, and the departure from the MTF of the diffraction-limited case is considerable even for a modest SA ($W_{40} = 0.5$). Beyond a moderate SA, the MTF contains zeros. When the hyper-Gaussian filter is used, the sensitivity of the MTF to SA is reduced as shown in figure 10. Although the magnitude of the MTF is considerably reduced in comparison to an ideal lens, it does not contain zeros even for SA as large as $W_{40} = 2$. There is a reduction of the

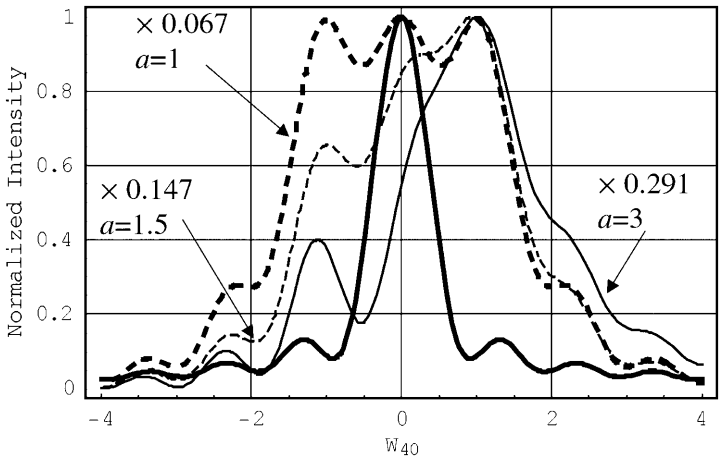

Figure 6. Normalized intensity at the focal point versus spherical aberration W_{40} for a clear circular aperture (——), and complex filter with $a = 1$, 1.5, and 3. The relative intensity scalings for the clear and two complex filters are indicated.

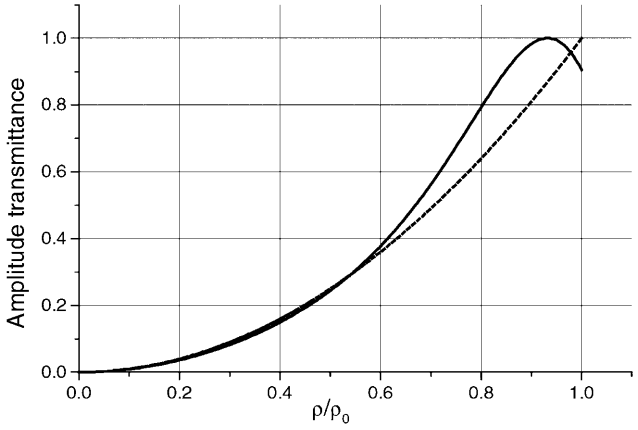

Figure 7. A comparison between the variation of the quadratic (- - - -) and the hyper-Gaussian transmittance as a function of the normalized radial coordinate.

effective cut-off frequency of about 5%, which will normally be unimportant. The recorded image can therefore be deconvolved to nearly the diffraction-limited case without a loss in information, but at the expense of a reduction in the signal-to-noise ratio.

2. Conclusions

We have derived combined amplitude and phase filters that enhance tolerance to SA but at the cost of a reduction in the transmitted optical power. The present design relies on the evaluation of the axial intensity by using the stationary phase approximation. The complex filters obtained can be implemented by the use of a two-dimensional programmable liquid-crystal spatial light modulator, as reported in [16].

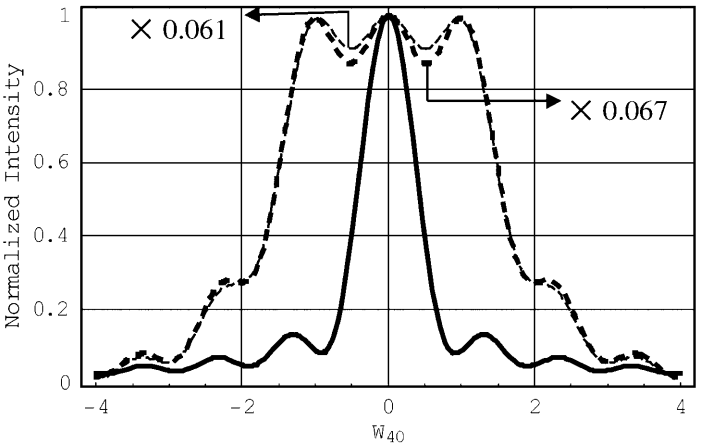

Figure 8. A comparison between the intensity at the focal point versus spherical aberration W_{40} for a circular aperture (——), the quadratic complex filter (- - - -), and the hyper-Gaussian complex filter (- - - -). The relative intensity scalings for the quadratic and hyper-Gaussian filters are indicated.

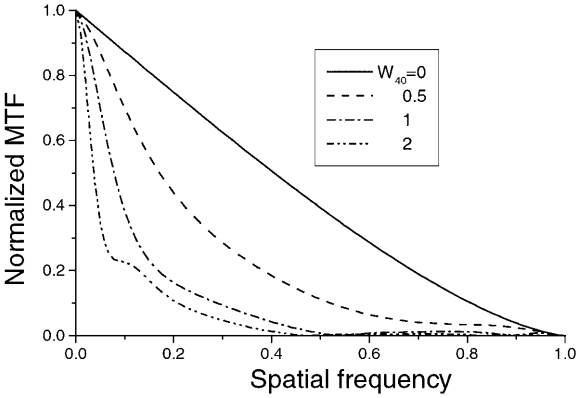

Figure 9. Normalized MTF of a perfect lens suffering from multiple spherical aberration $W_{40} = 0$, 0.5, 1, and 2.

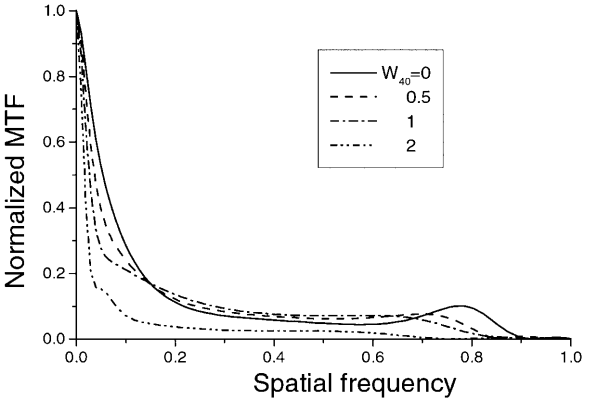

Figure 10. Normalized MTF of the hyper-Gaussain complex filter suffering from multiple spherical aberration $W_{40} = 0$, 0.5, 1, and 2.

Acknowledgment

This work was carried out with funding from the Sensors and Electronic Warfare Research Domain of the UK MoD Corporate Research Programme.

References

[1] Sheppard, C. J. R., 2000, *Appl. Opt.*, **39,** 6366.
[2] Karman, G. P., Van Dujil, A., and Woerdman, J. P., 1998 *J. Mod. Opt.*, **45,** 2513.
[3] Asakura, T., 1962, *Oyo Butsuri*, **31,** 243.
[4] Mino, M., 1971, *Appl. Opt.*, **10,** 2219.
[5] Yzuel, M. J., 1979, *Opt. Acta*, **26,** 1397.
[6] Sanyal, S., and Ghosh, A., 2002, *Appl. Opt.*, **41,** 4611.
[7] Ojeda-Castaneda, J., Andres, P., and Diaz, A., 1986, *Opt. Lett.*, **11,** 487.
[8] Ojeda-Castaneda, J., Andres, P., and Diaz, A., 1988, *J. Opt. Soc. Am. A*, **5,** 1233.
[9] Ojeda-Castaneda, J., Berriel-Valdos, L. R., and Montes, E., 1985, *Opt. Lett.*, **10,** 520.
[10] Ojeda-Castaneda, J., Tepichin, E., and Pons, A., 1988, *Appl. Opt.*, **27,** 5140.
[11] Ojeda-Castaneda, J., Tepichin, E., and Diaz, A., 1989, *Appl. Opt.*, **28,** 2666.
[12] Wang, H., and Gan, F., 2001, *Appl. Opt.*, **40,** 5658.
[13] Mezouari, S., and Harvey, A. R., 2003, *Opt. Lett.*, **28,** 771.
[14] Dowski, E. R., and Cathey, W. T., 1995, *Appl. Opt.*, **34,** 1859–1866.
[15] Zalvidea, D., and Sicre, E. E., 1998, *Appl. Opt.*, **37,** 3623–3627.
[16] Marquez, A., Iemmi, C., Escalera, J. C., Campos, J., Ledesma, S., Davis, J. A., and Yzuel, M. J., 2001, *Appl. Opt.*, **40,** 2316.